Mechanisms of innate events during skin reaction following intradermal injection of seasonal influenza vaccine

Jessica Gonnet, Lauranne Poncelet, Celine Meriaux, Elena Gonçalves, Lina Weiss, Nicolas Tchitchek, Eric Pedruzzi, Angele Soria, David Boccara, Annika Vogt, et al.

Manuscript number JPROT-D-19-00404

Mechanisms of innate events during skin reaction following intradermal injection of seasonal influenza vaccine

Jessica Gonnet[1#], Lauranne Poncelet[2,3#], Celine Meriaux[4#], Elena Gonçalves[1], Lina Weiss[1,5], Nicolas Tchitchek[6], Eric Pedruzzi[1], Angele Soria[1,7], David Boccara[1,8], Annika Vogt[1,5], Olivia Bonduelle[1], Gregory Hamm[3], Rima Ait-Belkacem[3], Jonathan Stauber[3], Isabelle Fournier[4], Maxence Wisztorski[4+] and Behazine Combadiere[1*+*].

[1]Sorbonne Université, Centre d'Immunologie et des Maladies Infectieuses – Paris (Cimi-Paris), INSERM U1135, Paris, France

[2] Univ. Lille, INSERM, CHU Lille, U1008 – Controlled Drug Delivery Systems and Biomaterials, F-59000 Lille, France

[3] ImaBiotech, 152 rue du Docteur Yersin, 59120 Loos, France

[4] Univ. Lille, Inserm, U1192 – Protéomique, Réponse Inflammatoire et Spectrométrie de Masse-PRISM, F-59000 Lille, France

[5] Clinical Research Center for Hair and Skin Science, Department of Dermatology and Allergy, Charité – Universitätsmedizin Berlin (2), 10117 Berlin, Germany

[6] CEA - Université Paris Sud 11 - INSERM U1184, Immunology of Viral Infections and Autoimmune Diseases, Institut de Biologie François Jacob, 92265 Fontenay-aux-Roses, France

[7] Service de Dermatologie et d'Allergologie, Hôpital Tenon, 4 rue de la Chine 75020 Paris, Hôpitaux Universitaire Est Parisien (HUEP), Assistance Publique Hôpitaux de Paris (APHP)

[8] Service de chirurgie plastique reconstructrice, esthétique, centre des brûlés, Hôpital Saint-Louis, Assistance Publique Hôpitaux de Paris (APHP), 1 avenue Claude Vellefaux, 75010 Paris, France

[#]: JG, LP, CM contributed equally to this work

[+]: MW and BC contributed equally to this work

*Corresponding author: Dr Béhazine Combadière, Centre d'Immunologie et des Maladies Infectieuses CIMI-Paris, 91 Boulevard de l'Hôpital, 75013 Paris, France. Phone: +33140779888, Fax: +33140779734, E-mail: behazine.combadiere@inserm.fr

Keywords: skin; biomarkers; Mass Spectrometry; intradermal vaccination; innate immunity

Running title: Skin biomarkers following intradermal immunization.

Funding sources: This project has received funding from the Agence National de Recherche (CE-16-0024-01). Behazine Combadière's laboratory has received funding from the Fondation pour la Recherche Médicale "Equipe FRM 2013" award.

Acknoweldgment: The authors are grateful to the Dormeur Foundation, and Vaduz for providing the Cryostat HM550 apparatus, to Juliette Masure (Imabiotech) for technical help in MALDI-FTICR processing and to Jo-Ann Cahn for English editing.

Conflicts of Interest: The authors have no financial conflicts of interest.

Abstract

The skin plays a crucial role in host defences against microbial attack and the innate cells must provide the immune system with sufficient information to organize these defences. This unique feature makes the skin a promising site for vaccine administration. Although cellular innate immune events during vaccination have been widely studied, initial events remain poorly understood. Our aim is to determine molecular biomarkers of skin innate reaction after intradermal (i.d.) immunization. Using an *ex vivo* human explant model from healthy donors, we investigated by NanoLC-MS/MS analysis and MALDI-MSI imaging, to detect innate molecular events (lipids, metabolites, proteins) few hours after i.d. administration of seasonal trivalent influenza vaccine (TIV). This multimodel approach allowed to identify early molecules differentially expressed in dermal and epidermal layers at 4 and 18 h after TIV immunization compared with control PBS. In the dermis, the most relevant network of proteins upregulated were related to cell-to-cell signalling and cell trafficking. The molecular signatures detected were associated with chemokines such as CXCL8, a chemoattractant of neutrophils. In the epidermis, the most relevant networks were associated with activation of antigen-presenting cells and related to CXCL10. Our study proposes a novel step-forward approach to identify biomarkers of skin innate reaction.

Abbreviations

APC: antigen-presenting cells

Dermal DCs: Dendritic cells

FTICR: Fourier-transform ion cyclotron resonance

i.d.: Intradermal

IPA: Ingenuity pathway analysis

KCs: Keratinocytes

LCs: Langerhans cells

LFQ: Label-free quantification

MALDI: Matrix assisted laser desorption ionization

MS: Mass spectrometry

MSI: Mass spectrometry imaging

PCA: Principal component analysis

TIV: Trivalent influenza vaccine

Introduction

The skin's outer surface acts like a suit, forming a physicochemical shield with specialized cells that scan and detect external molecules and danger signals. During barrier disruption (e.g., injuries, vaccination, drug injection), external stimuli reach the epidermal and dermal layer cells. Epidermal cells play a fundamental role in cutaneous innate immunity, providing both a physical barrier via tight junction formation of $CD45^{neg}$ keratinocytes (KCs), which constitute up to 90% of the epidermal cell population, alongside the scarcer Langerhans cells (LCs) (1-5% of epidermal cells) [1,2]. Other populations of antigen-presenting cells (APCs), such as dermal dendritic cells (dermal DCs), reside beneath the epidermal layer. Skin epithelial and resident APC subsets take part in antigen uptake and presentation to promote adaptive immunity in human and mouse models [2,3]. Skin barrier disruption provokes the local production of proinflammatory cytokines and chemokines by local skin cells including KCs, LCs, and dermal DCs. How these local resident cells are activated after barrier disruption, starting with the recruitment of inflammatory cells, determines the immunological outcome. However, the early *in situ* molecular biomarkers of skin reaction to this intrusion remain to be studied.

Our recent work has demonstrated that KCs respond to innate sensors and release IL-32, which allows LCs to detach from the epidermal layer, migrate to the dermis [4], and secrete proinflammatory chemokines and cytokines. These mediators promote inflammatory cell recruitment and APC activation [5–8]. This tissue reaction could reflect inflammatory processes necessary to bridge innate to adaptive immunity. In murine models, intradermal (i.d.) vaccination induces the attraction of neutrophils and monocytes to the immunization site [9,10]. However, initial molecular reaction at the site of immunization needs to be studied. In homeostatic and inflammatory skin tissues [2], several molecules such as mTORC1, the NLRP3 inflammasome, NF-kB signalling, and the MAPK/ERK pathway including EIF4/EIF2 factor transcription have been shown to regulate KCs proliferation and differentiation [11], maturation of skin APCs [12]. Here, we propose to use differential proteomic, lipidomic and metabolomic analysis using NanoLC-mass spectrometry/mass spectrometry (MS/MS) analysis and matrix assisted laser desorption ionization imaging (MALDI)-mass spectrometry imaging

(-MSI) to dissect the early molecular events following dermal immunization in a human skin explant model. Seasonal trivalent influenza vaccine (TIV) by i.d. route induces a potent local skin reaction and has been shown to be efficient in the induction of both humoral and T cell responses [13–16]. We thus planned to use TIV injection as a model antigen. We used an ex vivo human skin explant model, which has the advantage of conserving whole tissue architecture. The originality of this work is based on its spatio-temporal proteomic analysis of the epidermis and dermis at different time points after the inoculation. To our knowledge, this study is the first to use an *ex vivo* human skin explant model for a multiparametric analysis of proteins, lipids, metabolites, and mRNA to explore early cutaneous innate immune events before an inflammatory reaction to a vaccine at the inoculation site.

Material and methods

Human skin explants

Human skin samples were obtained from healthy volunteers (women aged 21-63 years) undergoing plastic surgery for breast, abdomen, or face lifts (Service de chirurgie plastique, reconstructrice et esthétique - Centre de traitement des brûlés, Saint-Louis Hospital, Paris, France). All skin samples were taken after informed consent in accordance with the local Institutional Ethics Committee guidelines (IRB 00003835) and the ethics rules stated in the Declaration of Helsinki. Skin samples were conserved in NaCl immediately after surgical excision and then processed within 4-6 hours post-surgery. They were examined macroscopically for tissue damage. Either PBS or Intanza® [TIV A/Michigan/45/2015 (H1N1)pdm09, A/Hong Kong/4801/2014 (H3N2), B/Brisbane/60/2008 -15 ug of haemagglutinin (HA)] (Sanofi-Pasteur, Lyon, France) was administered according to the Mantoux method by i.d. injection. In all, 45 µg of total HA protein/cm^2 of skin (volume: 25 µl of Intanza® and 15 µg of HA for each influenza strain) was injected in the dermis. Intanza formulation (100µL) was diluted to a quarter to be injected in each of the 1 cm^2 pieces of skin. Influenza vaccine and PBS control injected skin were incubated 4 and 18 h, draining in RPMI 1640 medium (Gibco® Thermo Fisher Scientific, Waltham, MA, U.S.A.). As Figure 1 shows, skin donors (n=6) were used both for cryosection for analysis by MALDI-Fourier-transform ion cyclotron resonance (-FTICR) and for epidermal and dermal cell suspensions for high throughput proteomic analysis. Skin samples were also used to validate cytokine and chemokine expression by qPCR (supplemental materials).

Skin epidermal and dermal layers

After the injections into fresh skin samples (1 cm^2), the tissue was cut into small pieces and incubated in RPMI 1640 medium with 2.4 IU/ml of dispase II (Sigma-Aldrich, St. Louis, MO, U.S.A.) overnight at 4°C with agitation to separate epidermal sheets from the dermis. Epidermal sheets were then removed from the dermis with mechanical tweezers. Epidermal cell suspensions were obtained after

10 minutes incubation at 37°C in RPMI 1640 and trypsin-EDTA 0.2% (Sigma-Aldrich), supplemented with DNase I (10 µg/mL, Roche, Boulogne Billancourt, France). Fetal calf serum (FCS, Dominique Dutscher, Brumath, France) was then added. Cell suspensions were washed in RPMI 1640 +20% FCS medium, processed through a 70-µm filter (Falcon BD™, San Jose, CA, U.S.A.), and then washed in PBS. Cell pellets were dried, then frozen and conserved at -80°C.

Protein detection and identification

See the supplementary information for the detailed protocol. Briefly, dermal and epidermal cells (the equivalent of 2 million cells for each condition) were lysed and proteins extracted with a Radioimmunoprecipitation assay (RIPA) buffer. Extracted proteins were digested with filter-aided sample preparation (FASP), and the peptides retrieved were analysed with a nanoUPLC system coupled with a high-resolution mass spectrometer for MS and MS/MS analysis. The detailed methods are described in the supplemental materials and methods section.

All MS data were processed with MaxQuant (version 1.5.6.5) by using the Andromeda search engine. The proteins were identified by searching MS and MS/MS data against the reviewed proteome for Homo sapiens in the UniProt database (Release February 2017, 20 172 entries) and 262 commonly detected contaminants. Trypsin specificity was used for digestion mode. N-terminal acetylation and methionine oxidation were selected as variable modifications and carbamidomethylation of cysteines as fixed. Up to two missed cleavages were allowed. An initial mass accuracy of 6 ppm was selected for MS spectra. The MS/MS tolerance was set to 20 ppm for the HCD data (higher-energy-collisional-dissociation). False discovery rates for peptide spectrum matches and for protein identifications were estimated by using a decoy version of the previously defined databases (reverse construction) and set at 1%. Relative label-free quantification (LFQ) of the proteins was conducted with MaxQuant, by applying the MaxLFQ algorithm with default parameters. Analysis of the identified proteins was performed with Perseus software (http://www.perseus-framework.org) (version 1.5.6.0). The file containing the information from the identification was used. Hits from the reverse database and proteins with only modified peptides were removed. Hits from potential contaminants were marked, and proteins originating from culture medium (e.g., serum albumin from Bos taurus) or sample

preparation (e.g., trypsin from Sus scrofa) were manually removed to ensure that only proteins that are part of the human skin structure were retained. LFQ intensities were transformed by base 2 logarithm before statistical analysis.

Statistical analysis

Protein expression data were analysed using R software. Analysis of the difference between TIV and PBS conditions at each time point was based on a paired nonparametric *t*-test (Wilcoxon signed-rank test), with a two-tailed test (p-value <0.05) considered a statistically significant. Unsupervised multivariate analysis was performed using Principal Component Analysis (PCA) using R software. Heatmaps and hierarchical clusters were generated with R software based on the Pearson coefficient of correlation with the complete linkage method.

Data availability statement. The normalized proteomic data that support the findings of this study have been deposited in ArrayExpress with the accession code XXXXX.

Results and Discussion

A multimodal approach of early innate events during skin reaction following intradermal injection of seasonal influenza vaccine

Using an *ex vivo* human skin explant model, we examined the cutaneous early innate molecular events induced at early time points (4 and 18 h) after TIV administration. Of note, skin explants is an ex vivo model that allows the investigation of early tissue reaction without inflammatory cells recruitment (absence of blood flow). We have previously showed that 3-4 hours after intradermal injection in the skin explants allows the detection of KC and LC activation to several intradermal stimuli (nanoparticle vaccine, modified vaccinia Ankara and Toll-like receptor ligands) [4,17]. We also showed LC renewal in the epidermis at 18 hours post i.d. injection of MVA [17] while inflammatory cells continue to migrate to the dermis [18]. We thus have chosen these time points for the further omics analysis. Figure 1a presents the experimental plan. Skin explants from 6 healthy donors were injected by i.d. route with either TIV or PBS. For each donor, we divided skin samples in two parts: 1) dermal and epidermal cell suspensions were prepared for protein identification with MS-based proteomics at 4 and 18 h after treatment; 2) skin tissue sections were cryopreserved for *in situ* analysis by MALDI-MSI of metabolite and lipid alteration (Figure 1a, flow chart, left branch). Results of LFQ proteomics were analysed to identify the significant proteins (that is, those with significantly differential expression) detected after TIV and PBS administration (Figure 1a, flow chart, right). Finally, we used the IPA program to explore networks and pathways (Figure 1a).

First, NanoLC-MS/MS analyses of dermal and epidermal cell suspensions allowed the identification of 2.375 common proteins. Principal Component Analysis (PCA) of all samples, restricted to this list of 2.375 proteins, separated the dermal and epidermal samples (Figure 1b). Accordingly, the dermal and epidermal samples differed significantly in their protein detection levels and were therefore studied separately. In addition, control skin incubated for 4 or 18 h after PBS

injection did not differ in protein detection levels at either time point, as PCA showed (Figure 1c). Additional analysis of the impact of age on protein distribution showed no difference between those individuals <35 years and >35 years (data not shown).

In the epidermis, we found 73 significant proteins detected at 4 h and 35 proteins at 18 h that were differentially expressed after TIV compared with PBS injection (Wilcoxon signed-rank test, *P*-value<0.05) (Figure 1d, Supplemental Table 1). In the dermis, we found 32 proteins at 4 h and 45 proteins at 18 h detected with significantly differential expression after TIV injection compared with PBS (Wilcoxon signed rank test, *P*-value<0.05) (Figure 1d, Supplemental Table 3). The Venn diagram in Figure 1d showed significant proteins, exclusive to the treatment condition and tissue layer with only few shared molecules, suggesting specific molecular events in each skin layer.

Identification of early inflammatory proteins and metabolites induced in the epidermis in response to i.d. TIV administration.

Heat-maps represent the detection levels of significant proteins (73 and 35 proteins differentially detected at 4 h and 18 h after treatment, respectively) in the epidermis of TIV-treated compared with PBS control skin at 4 and 18 h (Figures 2a and 2b, Supplemental Table 1). The PCA of all samples based on these proteins, separated TIV-treated from PBS control skin at both time points (Figure 2c, d).

We performed a functional enrichment analysis using Ingenuity Pathway Analysis (IPA), in order to understand the involvement of these proteins in immune functions. Supplemental Table 2 summarizes the top upregulated and downregulated proteins and their contributions to immune responses in the epidermis at, respectively, 4 h and 18 h. The Top IPA biological functions are cell-to-cell signalling and interaction (IPA: *P*-value = 1.53×10^{-3} - 4.75×10^{-2}), cellular assembly and organization (IPA: *P*-value = 3.39×10^{-4} - 4.31×10^{-2}), and immune cell trafficking (IPA: *P*-value = 2.41×10^{-3} - 4.05×10^{-2}). Among major proteins, IFITM3, STAT1, and IFI35 are involved in interferon signalling (IPA: *P*-value = 3.09×10^{-4}), while ICAM3 participates in cross-talk between cells (IPA: *P*-value = 3.2×10^{-4}) and PLCD1 with STAT1 in DC maturation (IPA: *P*-value = 4.75×10^{-3}) (Supplemental Table 2). STAT 1 is involved as well in the TH17 pathway, which is also a proposed outcome of skin immunization [4,17].

At 4 h after i.d. TIV administration, we detected the upregulation of ILK, LGALS1, SERPINB2, and IRF6, which are reported to contribute respectively to cutaneous wound contraction, wound healing, defects of the stratum corneum, and KC differentiation [19–22]. We also found the following proteins to be upregulated: IFI35, an inflammatory marker observed in skin lesions from atopic dermatitis [23], IFITM3, the expression of which increases on T cells after viral infection [24], and IRF6, which, driven by TLR3 activation, plays a role in KC cytokine expression [25]. Also notably upregulated were ICAM3 [26], HLA-B, and HLA-DRB5 [27] — all proteins allowing antigen presentation (IPA: *P*-value = 8.54×10^{-3}).

Supplemental Table 2 describes the proteins making major contributions to immune responses at 18 h. We found 9/35 proteins in the major IPA biological functions (Figure 2f). Most of these molecules were downregulated in the skin at 18 h (in green) and are involved in inflammatory responses (IPA: *P*-value = 1.73×10^{-3} - 2.10×10^{-2}), cell-to-cell signalling and interaction (IPA: *P*-value = 1.73×10^{-3} - $1.20\times1\ 0^{-2}$), cell movement (IPA: *P*-value = 1.73×10^{-3} - 1.89×10^{-2}), or macrophage functions (e.g., S100A10, HTT, MAPK13, PTPN6, GNG2, and MCAM) (IPA: *P*-value = 4.46×10^{-3} - 1.13×10^{-2}).

The protein networks significantly detected in the epidermis after TIV injection were connected to proinflammatory cytokines and chemokines, which we measured by qPCR analysis in epidermal cells before and after treatment. Figure 2g shows the mean gene expression in epidermal cell suspensions for 5 healthy donors. We observed significant increased expression of CX3CL1, CCL22, CXCL10, CXCL8, and TNFα genes at 4 h and 18 h after i.d. TIV injection.

Identification of early inflammatory proteins and metabolites induced in the dermis in response to i.d. TIV administration.

Significant detected proteins that are differentially expressed in the dermis for TIV-treated skin compared with PBS controls at 4 h and 18 h are represented in the heat maps (Figure 3a, 3b, respectively). In the dermis, we found 32 significant proteins detected differentially at 4 h and 45 proteins at 18 h after TIV compared with PBS injection (Supplemental Table 3). The PCA of all samples was based on the detection profiles of these genes, and the score plots showed that the

projections of PC1 (44.89% of the total variance for dermis 4 h and 48.10% for 18 h) and of PC2 (10.51 % for epidermis 4 h and 10.31% for 18 h) separated TIV-treated from PBS control skin for the dermal layer at both time points (Figure 3c, 3d). We performed a functional enrichment analysis using IPA for identification of top immunological pathways. Supplemental Table 4 summarizes the proteins that were upregulated and downregulated in the dermis in TIV-treated skin compared to PBS controls. These are mostly involved in cell-to-cell signalling and interaction (IPA: *P*-value = 6.29×10^{-3} - 2.19×10^{-2}) and interaction markers associated with skin inflammation (IPA Inflammatory Response: *P*-value = 4.72×10^{-3} - 2.34×10^{-2}). TRAF6 is one of them; its involvement in DC maturation (IPA: *P*-value = 3.43×10^{-2}) makes it an interesting biomarker of innate immunity for adaptive responses. Other downregulated molecules include EIF4B, which has been linked to mTOR signalling (IPA: *P*-value = 3.63×10^{-3}) and identified as an essential regulator in skin morphogenesis [28]. Interestingly, MYLK, a protein involved in cell morphology (IPA: *P*-value = 7.86×10^{-3} - 3.41×10^{-2}), was upregulated, and changes in the morphology of LCs but also DCs upon activation or danger signals are among the main features of skin APCs [17,2,12,4]. In the dermis, the production of some inflammatory markers was modified, including the well-known NFκB subunit and TRAF6 [29], as well as markers such as ITGB5 and HLA-A, which have been observed in particular in inflammatory skin disorders and cutaneous adverse reactions [30,31]. We also noted the upregulation of CD1a and the downregulation of CD207, markers that might account for the migration of LCs and CD207+ dermal DCs after their activation, respectively to the dermis and draining lymph nodes during cell trafficking [3,17]. Finally, PSMB4 and PSMD13, both proteins involved in the proteasome complex, which is crucial for antigen presentation, were also deregulated [32,33].

At 18 h, 11/45 molecules, all upregulated in TIV-treated skin, were involved in multiple mechanisms (Supplemental Table 4), such as cell signalling and interaction (IPA: *P*-value = 2.29×10^{-3} - 4.09×10^{-2}), cell repair (IPA: *P*-value = 2.29×10^{-3} - 4.92×10^{-2}), cell movement (IPA: *P*-value = 4.57×10^{-3} - 4.70×10^{-2}), injury (IPA: *P*-value = 2.29×10^{-3} - 4.72×10^{-2}), metabolism (IPA: *P*-value = 2.29×10^{-3} - 4.92×10^{-2}), molecular transport (IPA: *P*-value = 2.29×10^{-3} - 4.04×10^{-2}), and the cell cycle (IPA: *P*-value = 9.13×10^{-3} - 3.38×10^{-2}). These activities suggest massive reorganization and repair in the dermis — the site of injection of the vaccine compounds.

Because most of these molecules are also associated with inflammatory mediators, we measured the expression of the genes for these proinflammatory cytokines and chemokines, in connection with the protein network significantly detected by qPCR analysis of epidermal cells after TIV injection in the dermis. Figure 3g shows the mean gene expression in the dermal cell suspension in 5 healthy donors. We observed an increase in gene expression of CXCL10 at the early time points and of CCL22 and CXCL8 at 18 h after i.d. TIV administration.

Identification of major metabolites induced in the skin in response to i.d. TIV administration

As shown in figures 2 and 3, IPA pathways highlighted several metabolites and lipids potentially involved in top networks and may indicate changes in epidermal and dermal cellular processes. MALDI-FTICR has proved its efficacy in detection drug compounds and small molecules on skin explant tissue section imaging [34,35]. Using MALDI-FTICR, we performed *in situ* analyses on skin cryosections treated for 4 h compared with PBS controls (Supplemental Figure 1). The vaccine injection area was detected in the skin of 6 donors by a vaccine excipient, *i.e.* Octoxinol 10 (Supplemental Figure 1, left images). No detection of the vaccine excipient was found on PBS skin tissue section (right images). Based on IPA data base, metabolites and lipids potentially involved in top networks were analysed on tissue sections. As Figure 4a shows fold-changes of mean intensity of 8 metabolites and lipids (highlighted in IPA analysis), including phosphatidylcholine (PC) (32:0) and (36:1), phosphatidylinositol (PI) (34:1), diacylglycerol (DG) (34:1), adenosine diphosphate (ADP), linoleic acid (LA) (FA 18:2), phosphatidic acid (PA) (18:1), and sphingomyelin (SM) (d34:1), observed in TIV-treated skin compared to PBS controls, for each skin layer (Figure 4a). PA (18:1) (*P*-value = 0.049) and ADP or dGDP (*P*-value = 0.006) were overexpressed in the TIV condition and localized in the epidermis. Whereas LA (*P*-value = 0.05) was overexpressed in the TIV condition and localized in the dermis. PA (18:1) was overexpressed in the TIV condition and localized in the epidermis. Figure 4b shows the molecular distribution of PA (18:1) on skin and underlines that it was principally overexpressed in epidermis and at the top of the dermis. The molecular distribution of this lipid was homogenous inside the epidermis tissue. Figure 4c shows the molecular distribution of LA on each tissue. Mass spectrometry imaging (MSI) enabled the visualization of this compound's

overexpression in the dermis and epidermis. It is now well established that lipids and metabolites affect cutaneous innate immunity [36,37]. The mass spectrometric analyses showed the *in situ* modulation of metabolites and lipids related to proteins previously detected, such as MAPK3 and phospholipase D3 involved in immune signalling. Indeed, SM molecules detected in the dermis, are known to be related to such antimicrobial peptides as cathepsin B. Changes in SM and ceramide content have also been reported to affect membrane physiology directly, thus modifying signal transmission and interfering with diverse aspects of T cell activity [38]. For example, long-chain polyunsaturated fatty acids, such as LA (FA (18:2), have immunoregulatory functions via several mechanisms [39]. Some long-chain polyunsaturated fatty acids are precursors of lipid mediators [40], which participate in inflammatory processes and also affect acquired immune cells.

DG and PA, observed in the epidermis, have demonstrated links to signalling kinase proteins MAPK3. Moreover, DG can act as a second messenger to activate many downstream signalling cascades. DG has been an established ligand for protein kinase C isoforms that can influence inflammation [41,42]. We found additional dermal and epidermal molecules, detected by MALDI-MSI, such as LA, PC, ADP, and inositol phosphate detected *in situ*, thus demonstrating their effect in cutaneous immunity. Furthermore, PC in the form of several lipids, such as lysophosphatidic acid (LPA) (lysoPA), lysophosphatidylcholine (lysoPC), PI, and PA, has been observed to be expressed differentially in psoriasis patients compared with healthy volunteers [43]. Extracellular nucleotides such as ADP have also demonstrated their role in the regulation of DCs and of other immune cell functions, through their activation of some G-protein coupled receptors called P2 receptors or via ADP ribosylation, which increases the cAMP concentration [44]. Finally, inositol phosphate is reported to modulate the secretion of cytokines derived from both T and myeloid cells (IL-1β, IL-6, and IL-22) and TNF-α [45]. Accordingly, these mediators promote the recruitment of inflammatory cells such as neutrophils but also monocytes, which also play a role in the transport of antigens from the skin to the lymph nodes during inflammation; they also participate in CD8 T cell priming in the bone marrow and inflammatory signals in the lymph nodes [9,10,18,46] . LC activation in the epidermis and dermis consists of multiple events including CXCL10 production, morphological changes and down-regulation of cellular adhesion molecules, which are necessary for induction of adaptive immunity

412 both in human and murin models [4,18,47]. In humans, TIV vaccination by the i.d. route induced
413 systemic production of CXCL10, correlated with adaptive immune responses [15]. These
414 inflammatory mediators also promote APCs activation as well as T cell activation and polarization [5–
415 8].

416 In conclusion, to our knowledge, this study is the first to use an ex vivo human skin explant
417 model for a multiparametric analysis, combining several approaches to determine
418 modifications of metabolites, lipids, mRNA and proteins in response to cutaneous TIV
419 administration. We explored early local cutaneous innate immune events, in the different skin
420 layers, before any inflammatory reaction induced at the inoculation site. We found major
421 modifications in protein profiles that differentiated vaccine-injected skin from control
422 skin. These results add more insight into the molecular reaction in the skin that could be
423 involved in changes in the behavior of cells following i.d. injection. Indeed, we previously
424 showed that 4 hours after MVA i.d. injection, LCs migrate to the dermis as shown by decrease
425 in LC numbers, LC morphological changes (round shape LC) and CXCL10 production [17].
426 We also demonstrated these modifications are due to the release of IL-32 by keratinocyte
427 which down regulates KC-LC adhesion [4]. In addition, in murine models, we showed that
428 innate cell migration (neutrophils, inflammatory monocytes are detected in the skin between 4
429 and 8 hours following i.d. injection of MVA or nanoparticles [10,18]. In our work protein
430 networks are related to several cytokines/chemokines detected in the epidermis and dermis.
431 These inflammatory molecules could be related to DCs/LCs activation status (such as
432 CXCL10) which could orientate IFNγ-type responses or participates to CD4 T cell activation
433 (such as CXCL10 and CCL22). This later chemokine is the ligand of CCR4 and help in
434 positioning of T cell memory in the skin [48]. Neutrophils are attracted to the skin via
435 CXCL8, however we observed a significant increase in CXCL10 mRNA at 18 hours post-
436 injection and not at early time points (<4 hours). This could be either due to dichotomy

between either CXCL8 mRNA and protein secretion or the involvement of additional chemokines/chemokine receptors axis in early neutrophil trafficking [49]. We have also detected CX3CL1 mRNA suggesting initiation of monocyte trafficking to the skin. Finally, TNF-a could be involved in LC activation [50]. This study has demonstrated that proteomic analyses might enable the identification of potential early biomarkers of activated skin after vaccine administration by a cutaneous route.

References

[1] Combadiere B, Liard C. Transcutaneous and intradermal vaccination. Hum Vaccin 2011;7:811–27. https://doi.org/10.4161/hv.7.8.16274.

[2] Kabashima K, Honda T, Ginhoux F, Egawa G. The immunological anatomy of the skin. Nat Rev Immunol 2019;19:19. https://doi.org/10.1038/s41577-018-0084-5.

[3] Romani N, Thurnher M, Idoyaga J, Steinman RM, Flacher V. Targeting of antigens to skin dendritic cells: possibilities to enhance vaccine efficacy. Immunol Cell Biol 2010;88:424–30. https://doi.org/10.1038/icb.2010.39.

[4] Gonnet J, Perrin H, Hutton AJ, Boccara D, Bonduelle O, Mimoun M, et al. Interleukin-32 promotes detachment and activation of human Langerhans cells in a human skin explant model. Br J Dermatol 2018;179:145–53. https://doi.org/10.1111/bjd.16721.

[5] Berthier-Vergnes O, Bermond F, Flacher V, Massacrier C, Schmitt D, Péguet-Navarro J. TNF-α enhances phenotypic and functional maturation of human epidermal Langerhans cells and induces IL-12 p40 and IP-10/CXCL-10 production. FEBS Lett 2005;579:3660–8. https://doi.org/10.1016/j.febslet.2005.04.087.

[6] Krathwohl MD, Anderson JL. Chemokine CXCL10 (IP-10) is sufficient to trigger an immune response to injected antigens in a mouse model. Vaccine 2006;24:2987–93. https://doi.org/10.1016/j.vaccine.2005.11.032.

[7] Ouwehand K, Santegoets SJAM, Bruynzeel DP, Scheper RJ, Gruijl TD de, Gibbs S. CXCL12 is essential for migration of activated Langerhans cells from epidermis to dermis. Eur J Immunol 2008;38:3050–9. https://doi.org/10.1002/eji.200838384.

[8] Nedoszytko B, Sokołowska-Wojdyło M, Ruckemann-Dziurdzińska K, Roszkiewicz J, Nowicki RJ. Chemokines and cytokines network in the pathogenesis of the inflammatory skin diseases: atopic dermatitis, psoriasis and skin mastocytosis. Postepy Dermatol Alergol 2014;31:84–91. https://doi.org/10.5114/pdia.2014.40920.

[9] Abadie V, Bonduelle O, Duffy D, Parizot C, Verrier B, Combadière B. Original Encounter with Antigen Determines Antigen-Presenting Cell Imprinting of the Quality of the Immune Response in Mice. PLoS ONE 2009;4:e8159. https://doi.org/10.1371/journal.pone.0008159.

[10] Duffy D, Perrin H, Abadie V, Benhabiles N, Boissonnas A, Liard C, et al. Neutrophils Transport Antigen from the Dermis to the Bone Marrow, Initiating a Source of Memory CD8+ T Cells. Immunity 2012;37:917–29. https://doi.org/10.1016/j.immuni.2012.07.015.

[11] Buerger C, Shirsath N, Lang V, Berard A, Diehl S, Kaufmann R, et al. Inflammation dependent mTORC1 signaling interferes with the switch from keratinocyte proliferation

to differentiation. PloS One 2017;12:e0180853. https://doi.org/10.1371/journal.pone.0180853.
[12] Kashem SW, Haniffa M, Kaplan DH. Antigen-Presenting Cells in the Skin. Annu Rev Immunol 2017;35:469–99. https://doi.org/10.1146/annurev-immunol-051116-052215.
[13] Arakane R, Nakatani H, Fujisaki E, Takahama A, Ishida K, Yoshiike M, et al. Immunogenicity and safety of the new intradermal influenza vaccine in adults and elderly: A randomized phase 1/2 clinical trial. Vaccine 2015;33:6340–50. https://doi.org/10.1016/j.vaccine.2015.09.010.
[14] Gorse GJ, Falsey AR, Fling JA, Poling TL, Strout CB, Tsang PH. Intradermally-administered influenza virus vaccine is safe and immunogenic in healthy adults 18–64 years of age. Vaccine 2013;31:2358–65. https://doi.org/10.1016/j.vaccine.2013.03.008.
[15] Gonçalves E, Bonduelle O, Soria A, Loulergue P, Rousseau A, Cachanado M, et al. Innate gene signature distinguishes humoral versus cytotoxic responses to influenza vaccination. J Clin Invest 2019;129:1960–71. https://doi.org/10.1172/JCI125372.
[16] Marra F, Young F, Richardson K, Marra CA. A Meta-analysis of intradermal versus intramuscular influenza vaccines: Immunogenicity and Adverse Events: Meta-analysis of intradermal versus intramuscular influenza vaccines. Influenza Other Respir Viruses 2013;7:584–603. https://doi.org/10.1111/irv.12000.
[17] Liard C, Munier S, Joulin-Giet A, Bonduelle O, Hadam S, Duffy D, et al. Intradermal Immunization Triggers Epidermal Langerhans Cell Mobilization Required for CD8 T-Cell Immune Responses. J Invest Dermatol 2012;132:615–25. https://doi.org/10.1038/jid.2011.346.
[18] Levin C, Bonduelle O, Nuttens C, Primard C, Verrier B, Boissonnas A, et al. Critical Role for Skin-Derived Migratory DCs and Langerhans Cells in T FH and GC Responses after Intradermal Immunization. J Invest Dermatol 2017;137:1905–13. https://doi.org/10.1016/j.jid.2017.04.016.
[19] Li G, Li Y-Y, Sun J-E, Lin W, Zhou R. ILK–PI3K/AKT pathway participates in cutaneous wound contraction by regulating fibroblast migration and differentiation to myofibroblast. Lab Invest 2016;96:741–51. https://doi.org/10.1038/labinvest.2016.48.
[20] Lin Y-K, Yang S-H, Chen C-C, Kao H-C, Fang J-Y. Using Imiquimod-Induced Psoriasis-Like Skin as a Model to Measure the Skin Penetration of Anti-Psoriatic Drugs. PLoS ONE 2015;10. https://doi.org/10.1371/journal.pone.0137890.
[21] Schroder WA, Anraku I, Le TT, Hirata TDC, Nakaya HI, Major L, et al. SerpinB2 Deficiency Results in a Stratum Corneum Defect and Increased Sensitivity to Topically Applied Inflammatory Agents. Am J Pathol 2016;186:1511–23. https://doi.org/10.1016/j.ajpath.2016.02.017.
[22] Kwa MQ, Huynh J, Aw J, Zhang L, Nguyen T, Reynolds EC, et al. Receptor-interacting Protein Kinase 4 and Interferon Regulatory Factor 6 Function as a Signaling Axis to Regulate Keratinocyte Differentiation. J Biol Chem 2014;289:31077–87. https://doi.org/10.1074/jbc.M114.589382.
[23] Rebane A, Zimmermann M, Aab A, Baurecht H, Koreck A, Karelson M, et al. Mechanisms of IFN-γ-induced apoptosis of human skin keratinocytes in patients with atopic dermatitis. J Allergy Clin Immunol 2012;129:1297–306. https://doi.org/10.1016/j.jaci.2012.02.020.
[24] Wakim LM, Gupta N, Mintern JD, Villadangos JA. Enhanced survival of lung tissue-resident memory CD8⁺ T cells during infection with influenza virus due to selective expression of IFITM3. Nat Immunol 2013;14:238–45. https://doi.org/10.1038/ni.2525.
[25] Ramnath D, Tunny K, Hohenhaus DM, Pitts CM, Bergot A-S, Hogarth PM, et al. TLR3 drives IRF6-dependent IL-23p19 expression and p19/EBI3 heterodimer formation in keratinocytes. Immunol Cell Biol 2015;93:771–9. https://doi.org/10.1038/icb.2015.77.

[26] Manara GC, Pasquinelli G, Badiali-De Giorgi L, Ferrari C, Garatti SA, Fasano D, et al. Human epidermal Langerhans cells express the ICAM-3 molecule. Immunohistochemical and immunoelectron microscopical demonstration. Br J Dermatol 1996;134:22–7.
[27] Neefjes J, Jongsma MLM, Paul P, Bakke O. Towards a systems understanding of MHC class I and MHC class II antigen presentation. Nat Rev Immunol 2011;11:823–36. https://doi.org/10.1038/nri3084.
[28] Ding X, Bloch W, Iden S, Rüegg MA, Hall MN, Leptin M, et al. mTORC1 and mTORC2 regulate skin morphogenesis and epidermal barrier formation. Nat Commun 2016;7. https://doi.org/10.1038/ncomms13226.
[29] Matsumura T, Degawa T, Takii T, Hayashi H, Okamoto T, Inoue J, et al. TRAF6-NF-κB pathway is essential for interleukin-1-induced TLR2 expression and its functional response to TLR2 ligand in murine hepatocytes. Immunology 2003;109:127–36. https://doi.org/10.1046/j.1365-2567.2003.01627.x.
[30] Cretu D, Liang K, Saraon P, Batruch I, Diamandis EP, Chandran V. Quantitative tandem mass-spectrometry of skin tissue reveals putative psoriatic arthritis biomarkers. Clin Proteomics 2015;12. https://doi.org/10.1186/1559-0275-12-1.
[31] Okada Y, Han B, Tsoi LC, Stuart PE, Ellinghaus E, Tejasvi T, et al. Fine mapping major histocompatibility complex associations in psoriasis and its clinical subtypes. Am J Hum Genet 2014;95:162–72. https://doi.org/10.1016/j.ajhg.2014.07.002.
[32] Qureshi N, Perera P-Y, Shen J, Zhang G, Lenschat A, Splitter G, et al. The proteasome as a lipopolysaccharide-binding protein in macrophages: differential effects of proteasome inhibition on lipopolysaccharide-induced signaling events. J Immunol Baltim Md 1950 2003;171:1515–25. https://doi.org/10.4049/jimmunol.171.3.1515.
[33] Bi W, Zhu L, Zeng Z, Jing X, Liang Y, Guo L, et al. Investigations into the role of 26S proteasome non-ATPase regulatory subunit 13 in neuroinflammation. Neuroimmunomodulation 2014;21:331–7. https://doi.org/10.1159/000357811.
[34] Bonnel D, Legouffe R, Eriksson AH, Mortensen RW, Pamelard F, Stauber J, et al. MALDI imaging facilitates new topical drug development process by determining quantitative skin distribution profiles. Anal Bioanal Chem 2018;410:2815–28. https://doi.org/10.1007/s00216-018-0964-3.
[35] Sørensen IS, Janfelt C, Nielsen MMB, Mortensen RW, Knudsen NØ, Eriksson AH, et al. Combination of MALDI-MSI and cassette dosing for evaluation of drug distribution in human skin explant. Anal Bioanal Chem 2017;409:4993–5005. https://doi.org/10.1007/s00216-017-0443-2.
[36] Sawada Y, Honda T, Hanakawa S, Nakamizo S, Murata T, Ueharaguchi-Tanada Y, et al. Resolvin E1 inhibits dendritic cell migration in the skin and attenuates contact hypersensitivity responses. J Exp Med 2015;212:1921–30. https://doi.org/10.1084/jem.20150381.
[37] Sigmundsdottir H, Pan J, Debes GF, Alt C, Habtezion A, Soler D, et al. DCs metabolize sunlight-induced vitamin D3 to “program” T cell attraction to the epidermal chemokine CCL27. Nat Immunol 2007;8:285–93. https://doi.org/10.1038/ni1433.
[38] Beyersdorf N, Müller N. Sphingomyelin breakdown in T cells: role in activation, effector functions and immunoregulation. Biol Chem 2015;396:749–58. https://doi.org/10.1515/hsz-2014-0282.
[39] Carlsson JA, Wold AE, Sandberg A-S, Östman SM. The Polyunsaturated Fatty Acids Arachidonic Acid and Docosahexaenoic Acid Induce Mouse Dendritic Cells Maturation but Reduce T-Cell Responses In Vitro. PloS One 2015;10:e0143741. https://doi.org/10.1371/journal.pone.0143741.

[40] Sala-Vila A, Miles EA, Calder PC. Fatty acid composition abnormalities in atopic disease: evidence explored and role in the disease process examined. Clin Exp Allergy J Br Soc Allergy Clin Immunol 2008;38:1432–50. https://doi.org/10.1111/j.1365-2222.2008.03072.x.
[41] Mellor H, Parker PJ. The extended protein kinase C superfamily. Biochem J 1998;332 (Pt 2):281–92.
[42] Sharma A, Maurya CK, Arha D, Rai AK, Singh S, Varshney S, et al. Nod1-mediated lipolysis promotes diacylglycerol accumulation and successive inflammation via PKCδ-IRAK axis in adipocytes. Biochim Biophys Acta Mol Basis Dis 2019;1865:136–46. https://doi.org/10.1016/j.bbadis.2018.10.036.
[43] Zeng C, Wen B, Hou G, Lei L, Mei Z, Jia X, et al. Lipidomics profiling reveals the role of glycerophospholipid metabolism in psoriasis. GigaScience 2017;6. https://doi.org/10.1093/gigascience/gix087.
[44] Ferrari D, Gorini S, Callegari G, la Sala A. Shaping immune responses through the activation of dendritic cells–P2 receptors. Purinergic Signal 2007;3:99–107. https://doi.org/10.1007/s11302-006-9024-0.
[45] Lachmandas E, Rios-Miguel AB, Koeken VACM, van der Pasch E, Kumar V, Matzaraki V, et al. Tissue Metabolic Changes Drive Cytokine Responses to Mycobacterium tuberculosis. J Infect Dis 2018;218:165–70. https://doi.org/10.1093/infdis/jiy173.
[46] Abadie V. Neutrophils rapidly migrate via lymphatics after Mycobacterium bovis BCG intradermal vaccination and shuttle live bacilli to the draining lymph nodes. Blood 2005;106:1843–50. https://doi.org/10.1182/blood-2005-03-1281.
[47] Liard C, Munier S, Arias M, Joulin-Giet A, Bonduelle O, Duffy D, et al. Targeting of HIV-p24 particle-based vaccine into differential skin layers induces distinct arms of the immune responses. Vaccine 2011;29:6379–91. https://doi.org/10.1016/j.vaccine.2011.04.080.
[48] Alanio C, da Silva RB, Michonneau D, Bousso P, Ingersoll MA, Albert ML. CXCR3/CXCL10 axis shapes tissue distribution of memory phenotype CD8+ T cells in nonimmunized mice. J Immunol 2018;200:139–146.
[49] Kim CH, Kunkel EJ, Boisvert J, Johnston B, Campbell JJ, Genovese MC, et al. Bonzo/CXCR6 expression defines type 1–polarized T-cell subsets with extralymphoid tissue homing potential. J Clin Invest 2001;107:595–601.
[50] Cumberbatch M, Griffiths CE, Tucker SC, Dearman RJ, Kimber I. Tumour necrosis factor-alpha induces Langerhans cell migration in humans. Br J Dermatol 1999;141:192–200. https://doi.org/10.1046/j.1365-2133.1999.02964.x.

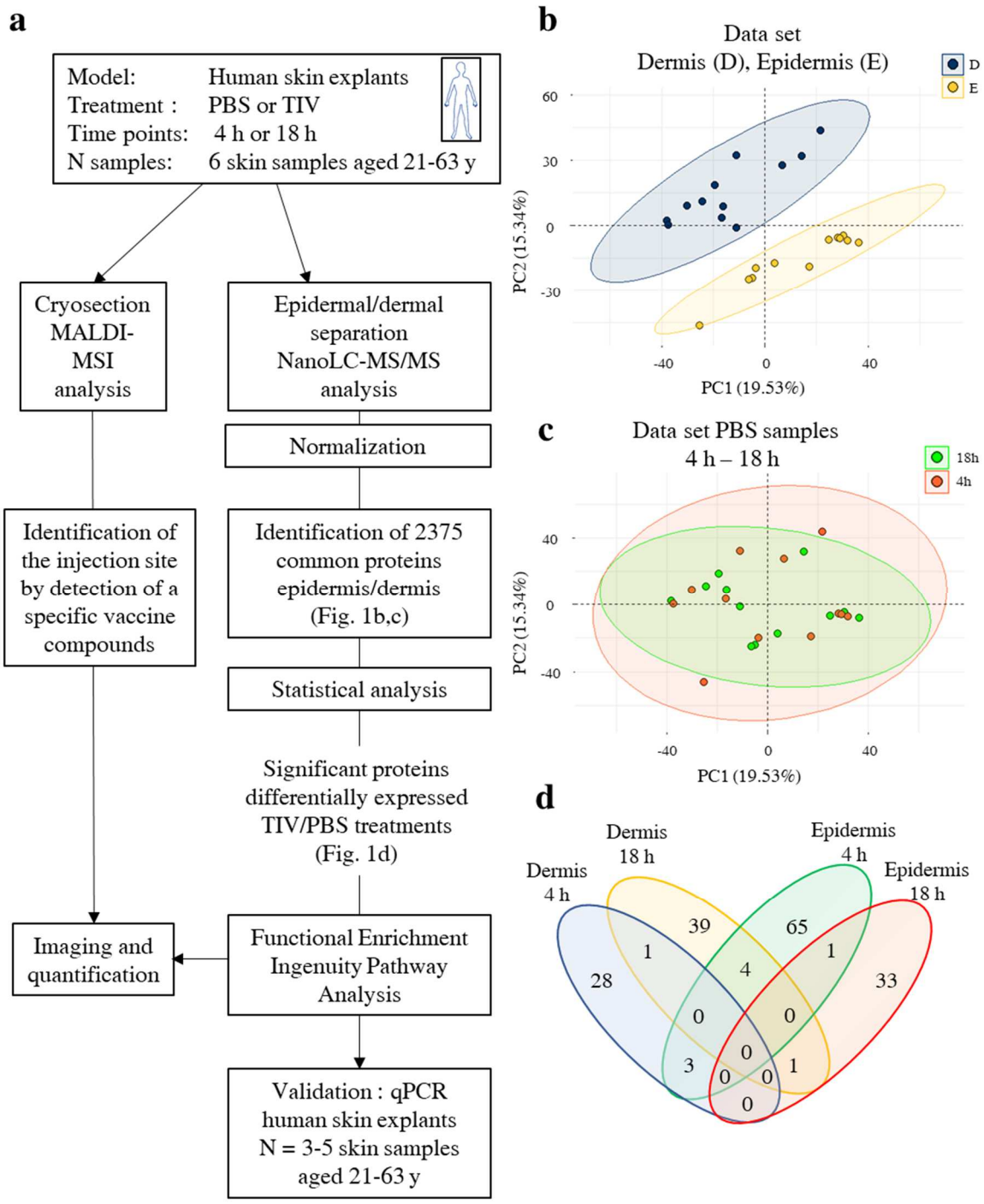

Figure 1: A multimodal approach of early innate events during skin reaction following intradermal injection of seasonal influenza vaccine

(a) **Flow Chart :** Human skin samples from six healthy donors (women aged 21-63 years), were cut into 1-cm^2 pieces after injection by TIV (Intanza®, microneedle device) or PBS by the i.d. route. Samples either underwent enzymatic digestion (flow chart, right) or cryopreservation (flow chart, left) for *in situ* investigation by MALDI-MSI of modifications in lipids and metabolites. Epidermal and dermal cell suspensions were used for proteomic analyses: the protein lysate was analysed by NanoLC-MS/MS; the peptide sequence analyses were processed by Maxquant software, and contaminants removed; and common proteins (n=2375) were identified in the epidermis and dermis after TIV and PBS administration. Following statistical analysis using Wilcoxon signed rank test, *P*-value<0.05. Statistical analyses were performed with R software (Wilcoxon matched-pairs signed rank test, with a two-sided *P*-value of <0.05). The Ingenuity Pathway Analysis (IPA) program was applied on significant proteins, to identify top gene networks and biological function. Gene expression was measured on mRNA samples extracted from the same donors (n=3-5 donors) by RT-qPCR. (b,c) Score plot from the PCA of all PBS samples based on the detection profiles of the 2375 proteins detected. (b) Projections of PC1 (19.53% of the total variance) and of PC2 (15.34%) separate the dermal (blue dots) and epidermal (yellow dots) samples defined by two concentration ellipses, (c) but do not separate 4 h (red dots) from 18 h (green dots) samples. (d) Venn diagram representing number of proteins significantly differentially detected in TIV compared to PBS in epidermis and dermis at 4 h and 18 h.

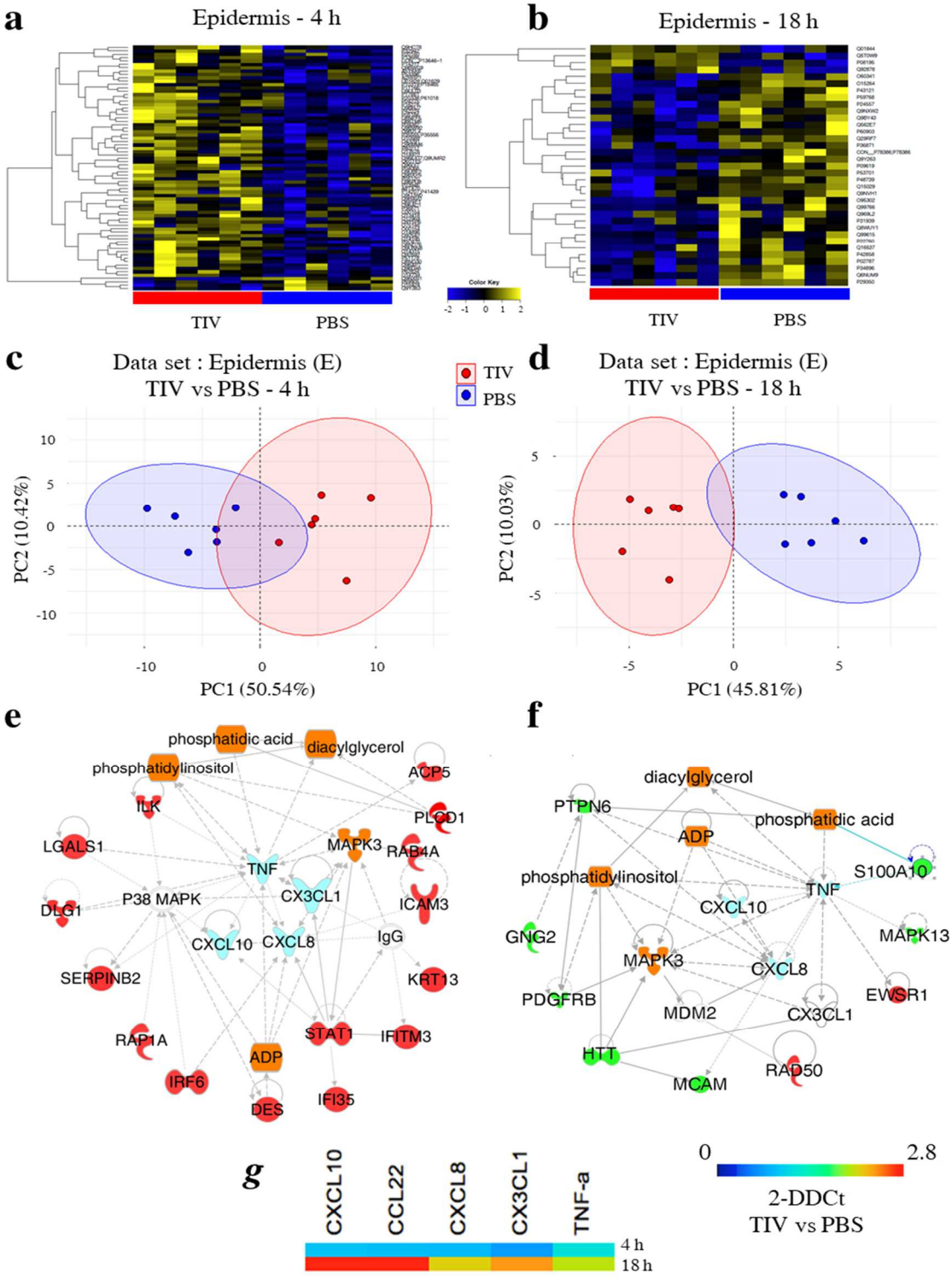

Figure 2: Identification of early inflammatory proteins and metabolites induced in the epidermis in response to i.d. TIV administration.

(a, b) Data set of significant proteins in the epidermis are represented in a heat-maps with the level of detection in TIV-treated compared to PBS-control skin at 4 h (a) and 18 h (b) (Wilcoxon matched-pairs signed rank test, *P*-value<0.05). (c,d) Score plots from the PCA are represented based on detection profiles of the 73 and 35 significant proteins differentially expressed between treated (red dots) and control (blue dots) samples at the 4 h condition (d) and 18 h (d) respectively. (e, f) Top networks from IPA highlighting major proteins from comparison of TIV and control conditions at 4 h (e) and 18 h (f). Overexpression after trivalent influenza vaccine (TIV) administration is represented in red, overexpression for the PBS condition in green. In orange the metabolites and lipids and in blue the proinflammatory cytokines found linked to the proteins of interest. In white, the proteins added by IPA, to complete the top network but not identified in our study. solid lines = direct relations, dashed lines = indirect relations. (g) mRNA expression analysis in epidermal cells injected with either TIV or PBS. Gene expression was normalized to the mean of actin and GAPDH expression and presented as relative fold gene expression levels compared to PBS controls, after calculating the 2^{-ddCt} values.

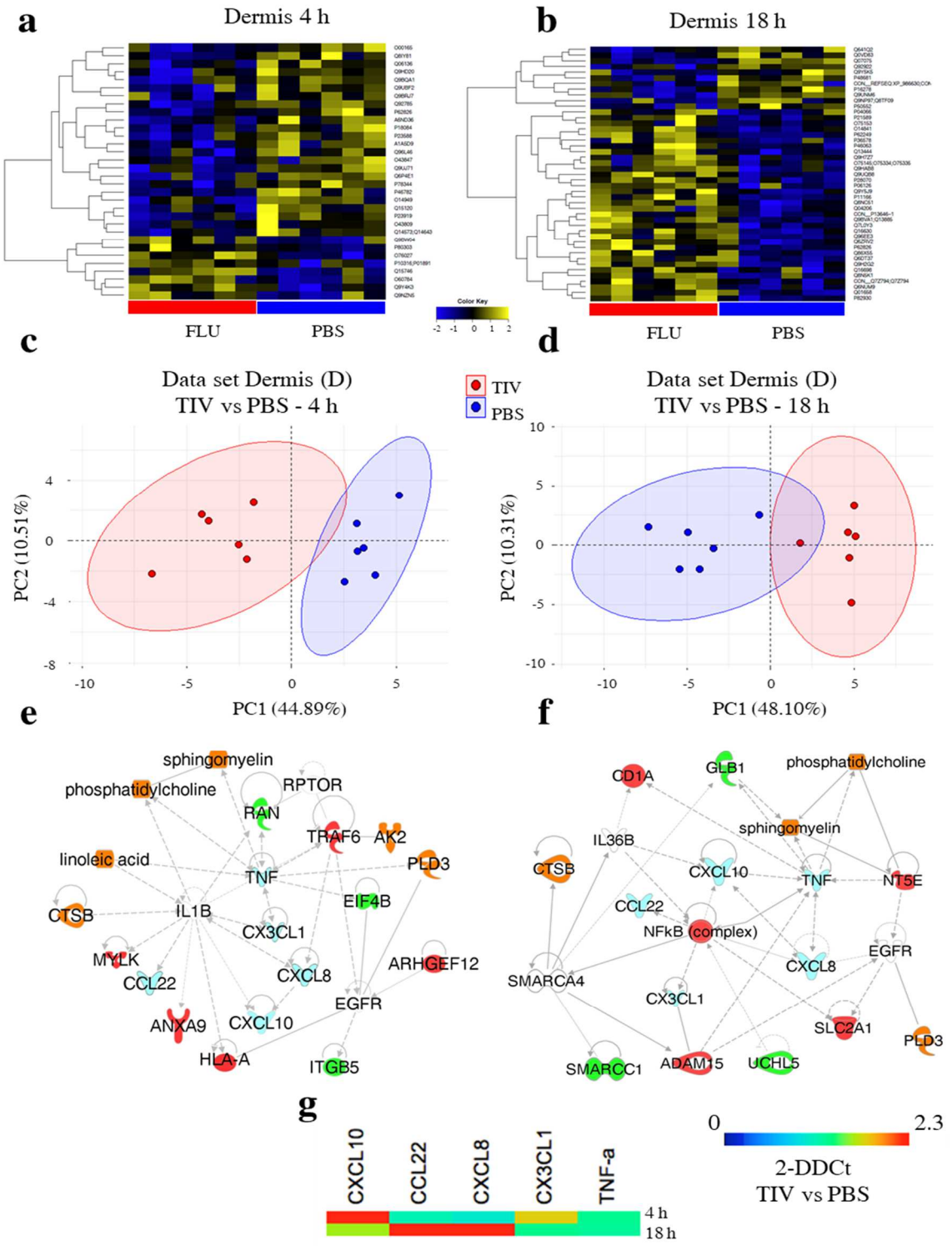

Figure 3: Identification of early inflammatory proteins and metabolites induced in the dermis in response to i.d. TIV administration.

(a, b) Data set of significant proteins in the dermis are represented in a heat-maps with the level of detection in TIV-treated compared to PBS-control skin at 4 h (a) and 18 h (b) (Wilcoxon matched-pairs signed rank test, *P*-value<0.05). (c,d) Score plots from the PCA are represented based on detection profiles of the 32 and 45 significant proteins differentially expressed between treated (red dots) and control (blue dots) samples at the 4 h condition (d) and 18 h (d) respectively. (e, f) Top networks from IPA highlighting major proteins from comparison of TIV and control conditions at 4 h (e) and 18 h (f). Overexpression after trivalent influenza vaccine (TIV) administration is represented in red, overexpression for the PBS condition in green. In orange the metabolites and lipids and in blue the proinflammatory cytokines found linked to the proteins of interest. In white, the proteins added by IPA, to complete the top network but not identified in our study. solid lines = direct relations, dashed lines = indirect relations. (g) mRNA expression analysis in epidermal cells injected with either TIV or PBS. Gene expression was normalized to the mean of actin and GAPDH expression and presented as relative fold gene expression levels compared to PBS controls, after calculating the 2^{-ddCt} values (n=3-5).

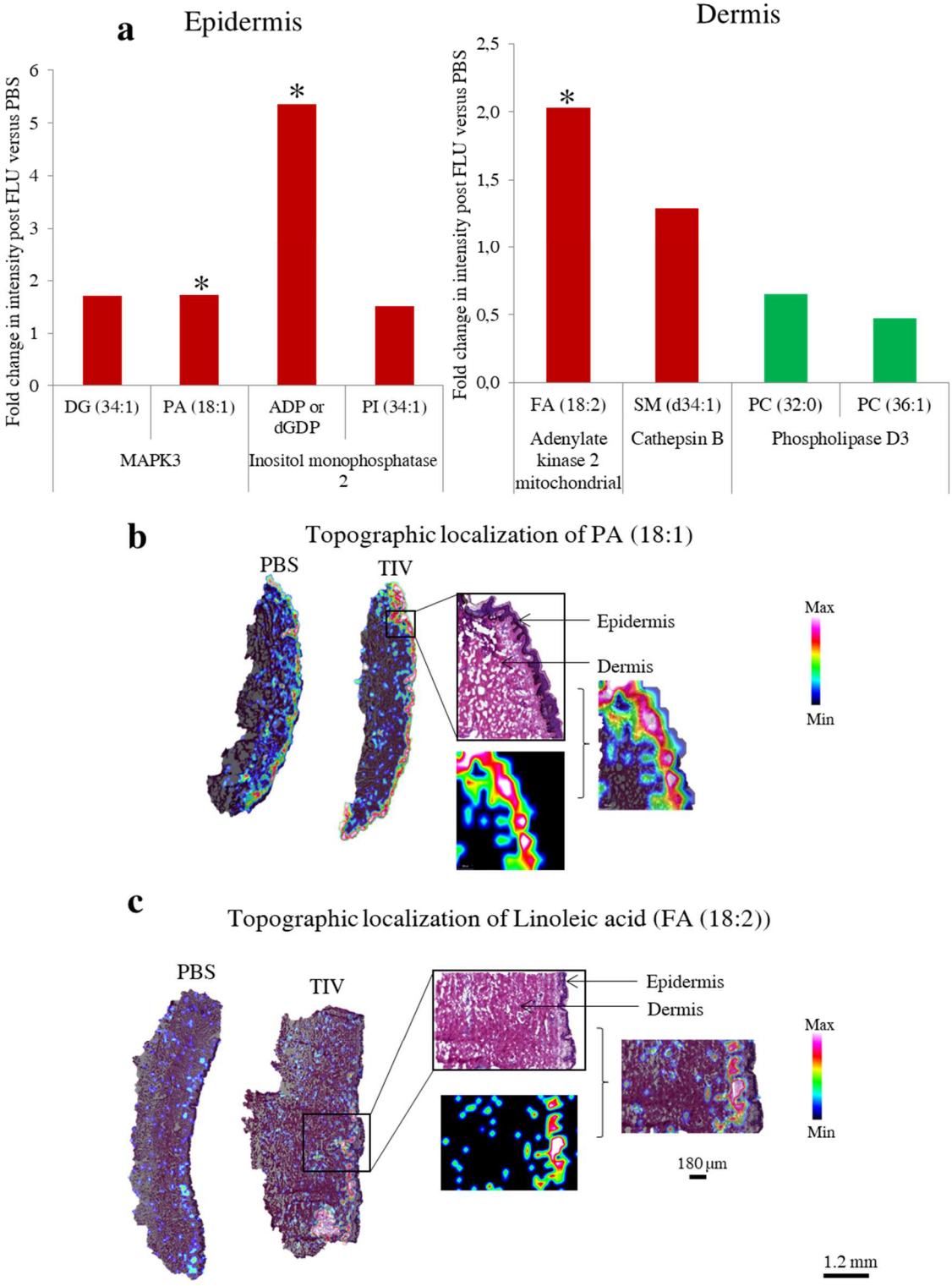

Figure 4: Identification of major metabolites induced in the skin in response to i.d. TIV administration
(a) Metabolites and lipids expression level in the epidermis (left) and in the dermis (right), according to IPA analysis. The fold changes of intensity were calculated comparing the TIV and PBS conditions. Overexpression after trivalent influenza vaccine (TIV) administration is represented in red, overexpression for the PBS condition in green. (b) Representative MALDI-MS imaging of PA (18:1) measured at *m/z* 435.2517 in TIV and PBS treated skins (c) Representative MALDI-MS imaging of Linoleic acid (FA 18:2) measured at *m/z* 279 in TIV and PBS treated skin. DG: diacylglycerol; ADP: adenosine 5′-diphosphate; dGDP: 2'-deoxyguanosine 5'-diphosphate; PI: phosphatidylinositol; LA: linoleic acid, FA: fatty acid; SM: sphingomyelin; PC: phosphatidylcholine.

Plastic surgery

Intradermal Trivalent Influenza vaccine (TIV) or PBS-treated human skin explant, incubated 4 or 18 h at 37ºC (10 cm^2)

Skin cryosections
6 donors

FLU

PBS

MALDI matrix deposition

MSI experiments

7T MALDI FTICR

Protein extraction & digestion from the epidermis (E) and the dermis (D)

NanoLC-MS/MS

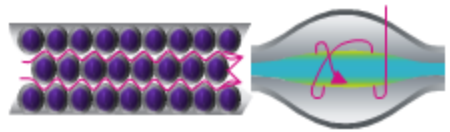

Omics analysis of the immunological system of skin tissue

Determination of zone of interest (vaccine compound localization)

TIV

PBS

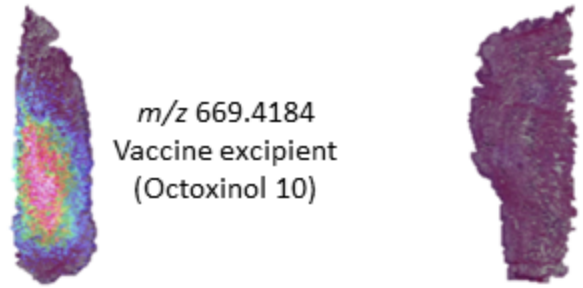

m/z 669.4184
Vaccine excipient
(Octoxinol 10)

Protein identification and bioinformatic analysis

Lipid and metabolite identification and bioinformatic analysis